



## Numerical simulation of a hybrid cogeneration-solar chimney power plant

Maryam Karami<sup>1,a</sup>, Morteza Khayam<sup>a</sup>

<sup>a</sup>Department of Mechanical Engineering, Faculty of Engineering, Kharazmi University, Tehran, Iran

Received: 2020-07-14

Accepted: 2020-08-31

### ABSTRACT

In this research, the effect of using the exhausted smoke of a cogeneration power plant as the working fluid of a solar chimney to increase power generation is studied by numerical methods. First, the cogeneration power plant is modeled using ASPEN HYSYS; then, the properties of the exhausted smoke including temperature, mass flow rate and etc. are entered to the model of solar chimney power plant, developed in ANSYS FLUENT. Using this hybrid model, the effect of solar radiation on power generation is compared for both air and smoke as working fluids. Furthermore, the effect of inlet temperature on power generation is also studied. The results showed that the power generation increases on average 4 times using smoke instead of air. It is also found that the optimum chimney height is 500 m using air and 600 m using the exhausted smoke of cogeneration power plant.

**Keywords:** Solar chimney power plant; Cogeneration power plant; Efficiency enhancement; Numerical simulation

### 1. Introduction

By growing the human need to the energy sources and the fossil fuel-related problems such as depletion and environmental pollution, the attention to the renewable energies has been enormously increased. One of the renewable energies that is available in different areas and at most hours of the day is solar energy. One of the simplest systems to harness solar radiation is the solar chimney power plant (SCPP), in which the air under a collector structure surrounding the central base of a very tall chimney tower is heated by solar radiation. As a result, a hot air updraft is caused in the tower, which drives turbine blades to produce electricity.

The effect of different parameters on the performance of the SCPP has been extensively studied [1-3]. Guo et al. [4] used the radiation model to simulate the air behavior inside the solar chimney. This model prevents the overestimation of the absorbed solar energy by the

chimney collector and predicts the acceptable pressure drop for turbine. The results showed that the effect of the ambient temperature on the power generation is insignificant. In the next study, they found that the optimum turbine pressure drop ratio varies from 0.90 to 0.94 for Spanish prototype under normal climate conditions [5]. Mehrpooya et al. [6] developed a 3D numerical model to investigate the energy and exergy performance of SCPP dynamically. Using Tehran climate data, they reported that the energy and exergy efficiencies changes from 3.50% to 93.3% and from 2.00% to 29.0%, respectively. Gholamzadeh and Kim [7] evaluated the performance of a solar chimney power plant using a titled collector roof. Using CFD analysis, an increase in the mass flow rate of the chimney has observed because of changing convection pattern.

Hu et al. [8] investigated the effect of a guide wall on the power output of a SCPP numerically and

\*corresponding author: [Karami@jhu.ac.ir](mailto:Karami@jhu.ac.ir)

experimentally. The key parameter was the height of the guide wall, which increases the mass flow rate inside the SCPP linearly and improves the driving force and power generation. This improvement was higher in the divergent chimney in comparison with the circular chimney.

Jiren et al. [9] evaluated the effect of chimney height, shape and collector size on the power generation. They developed a CFD model of the SCPP prototype in Manzanares, Spain and concluded that the increase of the chimney height and collector radius enhances the power generation of the SCPP. The effect of chimney design on its power generation is investigated by Nasraoui et al. [10]. Using CFD method, they considered the ratio of the chimney inlet and outlet diameter and both hyperboloid and conical chimney shape. Their results indicated that the efficient design is the hyperboloid chimney with higher power generation at the constant chimney height. Salehi et al. [11] introduced a new configuration of the SCPP, in which the outer concrete wall of conventional SCPP is replaced with a metal surface and also, the same volume of the wall is added to the absorber wall. They studied the effect of climatic conditions on the performance of the new SCPP and found that the new SCPP performs about 13%-20% better than the conventional one, especially in cold and dry climate zone.

In recent years, the performance of solar chimney power plant in combination with other thermal systems is widely studied by the researchers. Lee et al. [12] proposed an innovative combination of the SCPP with an organic Rankine cycle. The results showed that the required collector area of 41.0 m<sup>2</sup> provides the electricity demand of the buildings with 12 kWh/day. The combination of the SCPP and dry cooling tower has been investigated by Ghorbani et al. [13], in which the hot outlet gas of cooling tower is injected to the SCPP to maximize the power generation of the SCPP. Using this combination, the thermal efficiency of a 250 MW power plant increased about 0.5%. Using the same hybrid cooling-tower-solar-chimney system, Zhou and He [14] found that over 20 times increase in the power output of turbine is achieved. Andersen et al. [15] used a compost waste heat to enhance the performance of the SCPP. They reported that the proposed hybrid SCPP system has the potential of generating 100 MW with 83 M\$ annual saving. Fathi et al. [16] used the SCPP as the cooling tower of a nuclear power plant based on the steam Rankine cycle. They observed that the efficiency of the nuclear power plant decreases because of increasing the condenser temperature; however, the power generation of the SCPP increases. The total efficiency of the 1000 MW nuclear power plant

increases from 35.5% to 42%. Djimli et al. [17] combined the SCPP with a gas turbine to enhance the fluid inlet temperature to the SCPP. Using this combination, the power generation by the SCPP increased almost 10 times. Tian et al. [18] designed a hybrid SCPP, solid oxide electrolysis and fuel cell and optimized it using improved deer hunting algorithm. They used the cells for producing Hydrogen by the surplus solar radiation for the night time. Their results indicated that at the peak of radiation in Yazd, 0.16 kg/s hydrogen is produced. A photovoltaic (PV) panel integrated SCPP has proposed and studied by Singh et al. [19]. Based on the obtained results, the efficiency of PV panel enhanced 7% using a divergent chimney.

As reviews show, the combination of a SCPP with a cogeneration power plant (CPP) has not been investigated to date. Therefore, in this study, the exhausted smoke of a CPP is used as the working fluid of a SCPP. Furthermore, instead of using a heat exchanger to transfer the waste heat to the air flow, the smoke is directly entered into the chimney.

## 2. System description and modeling

In Figure 1, the schematic of a proposed combined system is shown, which has two main parts including a CPP and a solar chimney power plant. The CPP is a Brayton cycle based gas turbine power plant (UGT 25000), which has a compressor, a combustion chamber and a turbine, of which the exhausted smoke is entered to the collector of SCPP, as indicated in Figure 1. In the following section, the simulation of each system part has been explained.

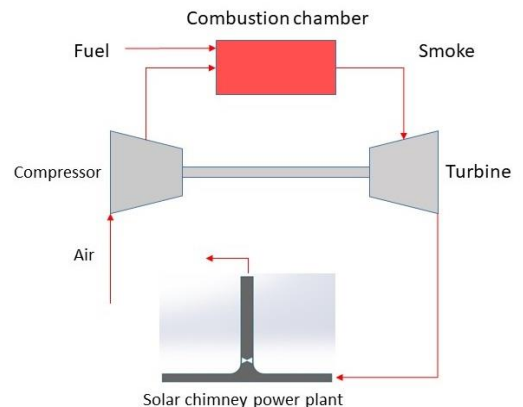


Figure 1. Schematic of a hybrid CPP-SCPP

### 2-1 CPP simulation

In this study, ASPEN HYSYS are used to simulate and analyze the cogeneration power plant, which is indicated in Figure 2. The various types of ASPEN HYSYS have been used to model the gas turbine cycle. The type of K100 is used for modeling the compressor and the type of CRV-100 is used for modeling the combustion chamber, in which the methane is completely burned. The compressed air from the compressor (arrow 2) and the methane (arrow 3) are mixed in the combustion chamber and burned. All reaction products are exited in gas phase from the combustion chamber (arrow 5) and there are no liquid products in the chamber outlet (the mass flow rate of arrow 6 is zero). The turbine is modeled using the type of K101. By entering the combustion gases (arrow 5) and the given turbine power, the properties of the exhausted smoke of turbine (arrow 7) have been calculated. For validating the developed model, the data of UGT 25000 such as pressure ratio and power generation, which is equal to 25 MW for this type of turbine, is entered into the model and the model outputs such as the temperature of the exhausted smoke and the fuel consumption rate per kWh are compared with the real data. The characteristic of UGT 25000 and the results of the simulation are shown in Table 1. As can be seen, the simulation error for the exhausted gas temperature is about 1.66% and for the fuel consumption is about 5.82%, which confirm the validation of the CPP simulation.

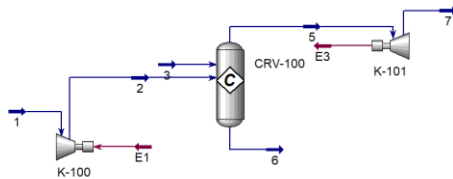


Figure 2. Schematic of a hybrid CPP-SCPP

Table 2. Characteristics of CPP (UGT 25000)

	Real data	Simulation data
Nominal power (kW)	25000	-
Electrical efficiency	35%	-
Fuel consumption (m3kWh)	0.275	0.291
Exhausted gas flow rate (kg/s)	87	-
Exhausted gas temperature	480	488
Dimensions (m)	6.4×2.5×2.7	-
Weight (ton)	16	-

### 2-2 SCPP simulation

In a solar chimney, the air flow is created by the natural convection because of indoor and outdoor air temperature difference, without the need for a mechanical device. For modeling the air flow inside the solar chimney, the following continuity, momentum and energy conservation equations should be solved simultaneously.

The continuity equation:

$$\frac{\partial \rho}{\partial t} + \nabla \cdot (\rho \vec{V}) = 0 \tag{1}$$

The momentum equation:

$$\rho \frac{d\vec{V}}{dt} = \rho \vec{g} - \nabla p + \nabla \cdot \tau_{ij} \tag{2}$$

The energy equation:

$$\rho \frac{\partial e}{\partial t} + p(\nabla \cdot \vec{V}) = \nabla \cdot (K\nabla T) + \Phi \tag{3}$$

The last term in Eq. (2),  $\tau_{ij}$ , is called Reynolds stress tensor and calculated using the following equation:

$$\tau_{ij} = \mu_t \left( \frac{\partial V_i}{\partial x_j} + \frac{\partial V_j}{\partial x_i} \right) - \frac{2}{3} \rho k \delta_{ij} \tag{4}$$

where,  $\delta_{ij}$  are the displacements in the different directions and  $\mu_t$  is the turbulent viscosity, which should be calculated using the average values, when the air flow is turbulent. For considering the flow regime in natural convection, a non-dimensional number called Rayleigh number is used:

$$Ra = \frac{g\beta(T_h - T_c)L^3}{\alpha\nu} \tag{5}$$

In this study, the k-ε two equation model is used for calculating the unknown in the Reynolds stress tensor:

$$\frac{\partial(\rho k)}{\partial t} + \text{div}(\rho k \vec{V}) = \text{div} \left( \frac{\mu_t}{\sigma_k} \nabla k \right) + 2\mu_t S_{ij} \cdot S_{jk} - \rho \epsilon \tag{6}$$

$$\frac{\partial(\rho \epsilon)}{\partial t} + \text{div}(\rho \epsilon \vec{V}) = \text{div} \left( \frac{\mu_t}{\sigma_\epsilon} \nabla \epsilon \right) + C_{1\epsilon} \frac{\epsilon}{k} 2\mu_t S_{ij} \cdot S_{jk} - \frac{C_{2\epsilon} \rho \epsilon^2}{k} \tag{7}$$

where k is the turbulent kinetic energy and ε is the turbulent viscous dissipation. By solving the k-ε equations,  $\mu_t$  can be calculated as follows:

$$\mu_t = \rho C_\mu \frac{k^2}{\epsilon} \tag{8}$$

In Eqs. (6), (7) and (8), five adjustable constants including  $\sigma_\epsilon$ ,  $\sigma_k$ ,  $C_{1\epsilon}$ ,  $C_{2\epsilon}$  and  $C_\mu$  should be given. Based on the previous studies [20], they assumed to be 1.3, 1, 0.09, 1.92 and 1.44, respectively.

For considering the effect of the temperature difference on the fluid density, the Boussinesq approximation is used:

$$(\rho - \rho_0)g \approx -\rho_0 g \beta (T - T_0) \tag{9}$$

where  $\beta(T-T_0) \ll 1$ ,  $\rho_0$  is the reference density at  $p_0$  and  $T_0$  and  $\beta$  is the thermal expansion coefficient of the air.

Finally, the mechanical power generated by the solar chimney using the pressure drop in the turbine and volumetric air flow rate is obtained as:

$$P_{mech} = \Delta p_t \times Q \tag{10}$$

For calculating the generated electrical power, the turbine electrical efficiency should be multiplied by the generated mechanical power.

In this study, the finite volume method (FVM) based on the ANSYS FLUENT software is used for solving the governing equations and simulation the air flow inside the solar chimney. The quadratic and structured meshing method as the best meshing type has been used for the geometry meshing. The grid independency analysis is performed by gradually reducing the mesh size and then, increasing the number of elements. The variation of the chimney outlet velocity versus the number of elements is shown in Figure 2. As observed, by increasing the number of elements to 200000, the variation of the outlet velocity is insignificant and thus, this mesh size is selected to consider the natural convection inside the chimney.

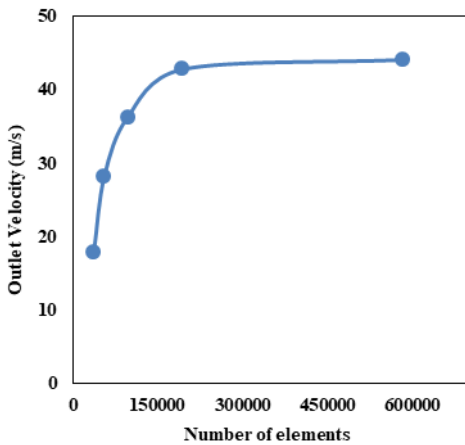


Figure 3. Grid independency analysis

The boundary conditions, used in this study, are indicated in Table 2. The incident solar radiation on the collector is assumed to be 1000 W/m<sup>2</sup>, of which 300 W/m<sup>2</sup> is absorbed by the collector. In other

words, the absorption coefficient of the ground is 0.3.

For considering the validity of the simulation, the chimney power generation for different chimney heights is plotted in Figure 4 and compared with the data from Ref. [21]. As can be seen, the simulation results are in good agreement with the results of Ref. [21].

Table 2. Boundary conditions used in the simulation

	Type	Description
Collector inlet	Pressure inlet	$T_0 = 293K, P_0 = 101325Pa$
Collector roof	Wall	With natural convection and without heat flux
Ground	Wall	Heat flux = 300 W/m <sup>2</sup>
Chimney outlet	Pressure outlet	Ambient condition (pressure and temperature) at the elevation of chimney outlet
Turbine blades	Wall	Moving relative to the adjacent zone

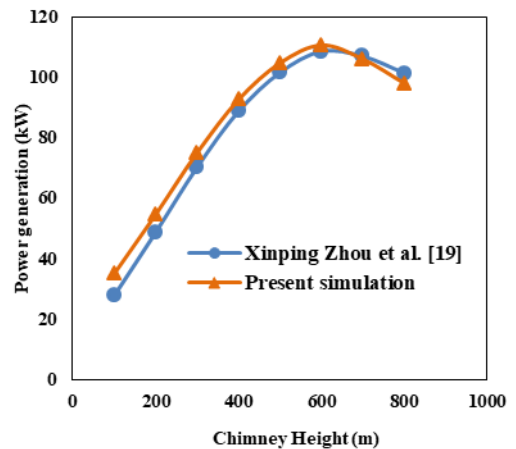


Figure 4. Validation of the simulation results

### 3. Results and discussion

In Figure 5, the effect of solar radiation on the power generation by the solar chimney is shown for different working fluids. As the absorbed radiation increases, the absorber surface becomes warmer and the air near it becomes warmer. This reduces the air density and the formation of upward flow. Because of the warmer surface, the speed of upward flow also increases.

It is also found from Figure 5 that the variation of the power generation by the solar radiation is linear

for both air and smoke; however, the power generation is higher using smoke as the working fluid because of the higher temperature of the inlet smoke.

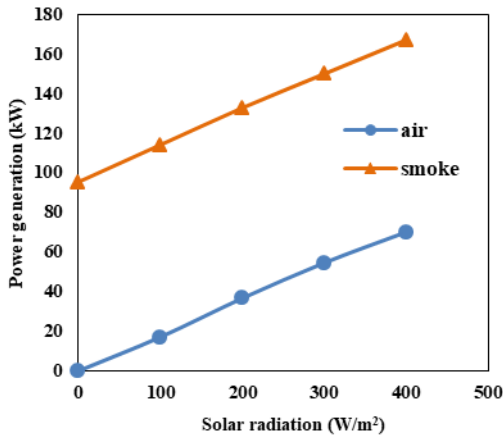


Figure 5. Effect of solar radiation on the chimney power generation

It is interesting to note that the power generation is different when the solar radiation is zero. Using air as the working fluid, the generation power is zero, whereas it is about 100 W/m<sup>2</sup> using smoke as the working fluid. It is because the outlet smoke from CPP has the high temperature; therefore, the solar chimney generates power even when the solar radiation is zero. It can be concluded that by using CPP exhausted smoke as the working fluid, the power generation significantly increases both during the day and at night or cloudy days, in which the solar radiation is small.

The variation of the chimney power generation by the flow rate is indicated in Figure 6. Because the flowrate of the outlet smoke from each CPP unit is constant, the smoke flowrate increases by increasing the number of CPP units from 1 (87 kg/s) to 5 (435 kg/s). As seen, the power generation increases linearly by the flowrate for both air and smoke. At the same flowrate, the power generation using smoke is significantly higher than that using air, because of the higher temperature. However, the air flow from the environment around the chimney is not limited; therefore, the power generation of the chimney by the unlimited air flowrate is 54.6 kW, which is 13.73% higher than that (47.1 kW) by the smoke flowrate of 87 kg/s, because the outlet smoke of one CPP unit is limited. Using the smoke of at least two CPP units generates the power of about 180 kW, which is higher than that using the air flow. This reveals that the number of CPP units and the

operating period plays a key role in the thermal performance of the combined CPP-chimney system.

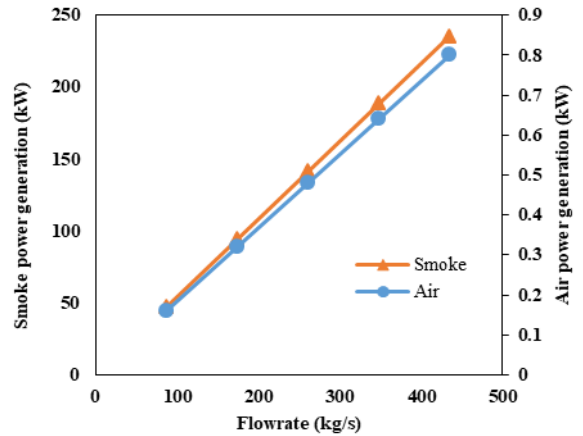


Figure 6. Effect of the flowrate on the chimney power generation

Figure 7 shows the effect of the inlet temperature on the power generation. The results show that the power generation increases by inlet temperature using both air and smoke as the working fluids. By increasing the inlet temperature, the air density reduces and as a result, the air upward speed inside the chimney enhances. For every 5 °C and 0.5 °C increase in respectively air and smoke inlet temperature, the power generation has increased by up to 1%.

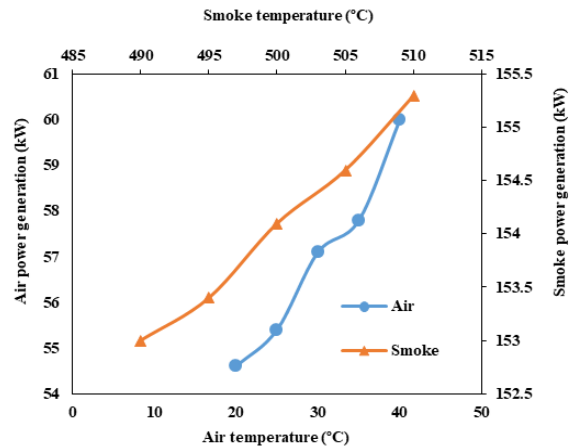


Figure 7. Effect of the inlet temperature on the chimney power generation

The variation of the power generation by the chimney height is depicted in Figure 8. Assuming the constant collector area and chimney diameter, the chimney height has increased from 200 m to 600 m with the step of 100 m. As can be seen, up to a chimney height of 400 m, with 100

m increasing the chimney height the power generation increases by 40% using air and by 10% using smoke. Generally, the temperature difference and therefore, the pressure difference between the chimney inlet and outlet become more significant. This results in the system performance enhancement and larger power output.

Looking Figure 8, it is interesting to note that the power output increases by the chimney height asymptotically and then, decreases. It is because the friction wall increases by increasing the height, which causes the reduction of power generation due to the pressure drop and back flow. Consequently, the optimum chimney height is 500 m using air and 600 m using CPP smoke. There is another limiting factor to increase the chimney height, and that is the increase in stresses at the base of the chimney due to tall height [22].

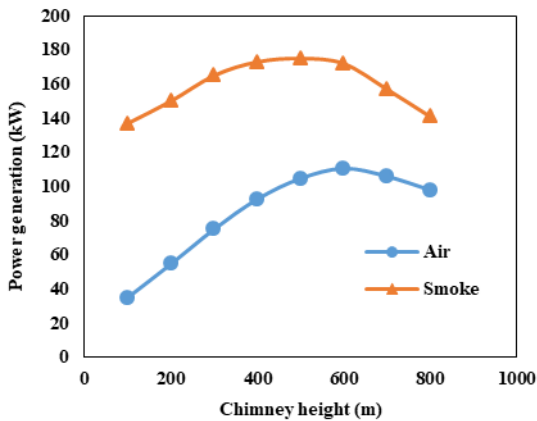


Figure 8. Effect of the chimney height on the chimney power generation

#### 4. Conclusion

In this paper, the performance of a SCPP in combination with a CPP is numerically investigated. The findings can be summarized as follows:

- For both working fluids (air and smoke), for every 100 W/m<sup>2</sup> of increased solar radiation, the power generation is 2.15 times. This shows the significant effect of the solar radiation on the SCPP performance.
- By increasing the flow rate, the power generation increases. At the same flow rate, using smoke instead of air, the power generation increases 2.75 times.
- For every 5°C increase in air temperature and for every 0.5°C increase in smoke temperature, the electricity generated in the chimney increases by up to 1%.
- Up to a height of 400 m, per 100 m of chimney height increase, the power generation increases by about 40% using air and by 10% using smoke. From the height of the 400 m and above,

the rate of increase in the power generation has decreased so that by changing the height from 500 m to 600 m, the power generation experiences only a 3% increase. The optimum chimney height is 500 m using air and 600 m using CPP exhausted smoke. Increasing the chimney height to more than 600 m does not have a positive effect on power generation and may have the opposite effect, because of the larger friction loss.

#### Nomenclature

$C_{1\varepsilon}$ : Constant in k- $\varepsilon$  equations  
 $C_{2\varepsilon}$ : Constant in k- $\varepsilon$  equations  
 $C_{\mu}$ : Constant in k- $\varepsilon$  equations  
 $e$ : Specific energy, J/kg  
 $g$ : Gravitational acceleration, 9.81 m/s<sup>2</sup>  
 $G_k$ :  
 $G_b$ :  
 $K$ : Thermal conductivity, W/m.K  
 $k$ : Turbulent kinetic energy, J  
 $L$ : Characteristic length, m  
 $p$ : Pressure, Pa  
 $P$ : Power, W  
 $Q$ : Volumetric flow rate, m<sup>3</sup>/kg  
 $Ra$ : Rayleigh number  
 $t$ : Time, s  
 $T_c$ : Inlet air temperature, K  
 $T_h$ : Outlet air temperature, K  
 $V$ : Velocity, m/s  
 $x$ : Coordinate, m

#### Greek symbols

$\rho$ : density (m<sup>3</sup>/kg)  
 $\mu$ : Dynamic viscosity, Kg/m.s  
 $\nu$ : Kinematic viscosity, m<sup>2</sup>/s  
 $\alpha$ : Thermal diffusivity, m<sup>2</sup>/s  
 $\beta$ : Thermal expansion coefficient, 1/K  
 $\nabla$ : Gradient operator  
 $\tau$ : Stress, Pa  
 $\delta$ : Displacement, m  
 $\varepsilon$ : Turbulent viscous dissipation,  
 $\Phi$ : Viscous dissipation  
 $\sigma_k$ : Constant in k- $\varepsilon$  equations  
 $\sigma_\varepsilon$ : Constant in k- $\varepsilon$  equations

## References

1. Ming, T., Wu, Y., K.de\_Richter, R., Liu, W., Sherif, S.A., *Solar updraft power plant system: A brief review and a case study on a new system with radial partition walls in its collector*, Renewable and Sustainable Energy Reviews, 2017. **69**: p. 472-487.
2. Guo, P., Li, T., Xu, B., Xu, X., Lia J., *Questions and current understanding about solar chimney power plant: A review*, Energy Conversion and Management, 2019. **182**, p. 21-33.
3. Arzpeyma, M., Mekhilef, S., Md. Salim Newaz, K., Horan, B., Seyedmahmoudian, M., Akram, N., Stojcevski, A., *Solar chimney power plant and its correlation with ambient wind effect*, Journal of Thermal Analysis and Calorimetry volume, 2020. **141**: 649–668.
4. Guo, P., Li, J., Wang Y., *Numerical simulations of solar chimney power plant with radiation model*, Renewable energy, 2014. **62**: p. 24-30.
5. Guo, P., Li, J., Wang Y., Wang Y., *Evaluation of the optimal turbine pressure drop ratio for a solar chimney power plant*, Energy conversion and management, 2016. **108**: p.14-22.
6. Mehrpooya, M., Shahsavan, M., Sharifzadeh, M.M.M., *Modeling, energy and exergy analysis of solar chimney power plant-Tehran climate data case study*. Energy, 2016, **115**: p. 257-273.
7. Gholamalizadeh, E., Kim M., *CFD (computational fluid dynamics) analysis of a solar-chimney power plant with inclined collector roof*, Energy, 2016. **107**: p.661-667.
8. Hu, S., Leung, D.Y.C., Chen, M.Z.Q., Chan, J.C.Y., *Effect of guide wall on the potential of a solar chimney power plant*, Renewable energy, 2016. **96**: p. 209-219.
9. M. Jiren, R. Bhoraniya, A. Harichandan, *CFD analysis of solar chimney power plant: Effect of chimney height, shape and collector size*, 4, 1, 2019, 61-71.
10. Nasraoui, H., Driss, Z., Kchaou, H., *Effect of the chimney design on the thermal characteristics in solar chimney power plant*, Journal of Thermal Analysis and Calorimetry, 2020. **140**: p. 2721–2732.
11. Salehi, A., Delfani, S., Karami, M., Bozorgi, M., *The effect of climatic conditions on the performance of a new configuration of solar chimney*, 2020. **5** (1): p. 332-340.
12. Lee, D.S., Hung, T.C, Lin, J.R., Zhao, J., *Experimental investigations on solar chimney for optimal heat collection to be utilized in organic Rankine cycle*, Applied energy, 2015. **154**: p. 651-662.
13. Ghorbani, B., Ghashami, M., Ashjaee, M., Hosseinzadegan, H., *Electricity production with low grade heat in thermal power plants by design improvement of a hybrid dry cooling tower and a solar chimney concept*. Energy conversion and management, 2015. **94**: p. 1-11.
14. Zou, Z., He, S., *Modeling and characteristics analysis of hybrid cooling-tower-solar-chimney system*, Energy Conversion and Management, 2015. **95**: p. 59–68.
15. Anderson, K.R., Salem, Y., Shihadeh, S., Perez, P., Kampen, B., Jouhar, S., Bahrani, S., Wang, K., *Design of a Compost Waste Heat to Energy Solar Chimney Power Plant*, Journal of Civil Engineering Research, 2016. **6**: p. 47-54.
- [16] Fathi, N., McDaniel, P., Aleyasin, S.S., Robinson, M., Vorobieff, P., Rodriguez, S. Oliveira, S., *Efficiency enhancement of solar chimney power plant by use of waste heat from nuclear power plant*, Journal of cleaner production, 2018. **180**: p. 407-416.
17. Djimli, S., Chaker, A., Ajib, S., Habka, M., *Studying the possibility of a combined hybrid solar chimney power plant with a gas turbine*, Environmental Progress and sustainable energy, 2018. **37** (3): p.1160-1168.
18. Tian, M., Yan, S., Han, S., Nojavan, S., Jermittiparsert, K., Razmjooyd, N., *New optimal design for a hybrid solar chimney, solid oxide electrolysis and fuel cell based on improved deer hunting optimization algorithm*, Journal of Cleaner Production, 2020. **249**: 119414.
19. Pratap, A., Kumar, S.A., Akshayveer, Singh, O.P., *Performance enhancement strategies of a hybrid solar chimney power plant integrated with photovoltaic panel*, Energy Conversion and Management, 2020. **218**: 113020.
20. Kasaeian, A., Mahmoudi, A.R., Razi Astaraei, F., Hejab, A., *3D simulation of solar chimney power plant considering turbine blades*, Energy Conversion and Management, 2017. **147**: p. 55-65.
21. Zhou, X., Yang, J., Xiao, B., Hou, G., Xing, F., *Analysis of chimney height for solar chimney power plant*, Applied Thermal Engineering, 2009. **29**(1): 178-185.
22. Harte, R. and G.P. Van Zijl, *Structural stability of concrete wind turbines and solar chimney towers exposed to dynamic wind action*, Journal of Wind engineering and industrial aerodynamics, 2007. 95(9-11): p. 1079-1096.